Contribution from the Department of Chemistry and Biochemistry, University of Notre Dame, Notre Dame, Indiana 46556,
Faculty of Pharmaceutical Sciences, Nagoya City University, Mizuho-Ku, Nagoya 467, Japan,
and Department of Chemistry and Biochemistry, San Francisco State University, San Francisco, California 94132

Models of Cytochromes b. Attempts to Control Axial Ligand Orientation with a "Hindered" Porphyrin System

Keiichiro Hatano,*[,1,2] Martin K. Safo,[1] F. Ann Walker,*[,3] and W. Robert Scheidt*[,1]

The interaction of imidazole ligands with the sterically hindered porphyrin derivative (perchlorato)(tetrakis(2,6-dichlorophenyl)porphinato)iron(III), [Fe(T2,6Cl₂PP)(OClO₃)], has been investigated. Measurements of stepwise ligand binding constants for 1-vinyl-, 1-methyl-, and 2-methylimidazole yield derived values of log β'_2 of 7.41, 5.16, and 7.12, respectively. These values clearly show that the eight *o*-chloro groups do not hinder the binding of the axial imidazole ligands. The preparation of the bis(1-vinylimidazole)iron(III) derivative is reported. This six-coordinate low-spin complex is found to display an unusual electron paramagnetic resonance spectrum in the solid state where both a "normal rhombic" and a "large g_{max}" EPR signal are observed at 7 K. The frozen solution spectrum shows only the rhombic signal. The crystal structure, determined at 122 ± 3 K, shows two different relative orientations of the axial imidazoles: "parallel" and "perpendicular". The observed perpendicular orientation is the one in which the axial imidazoles lie close to adjacent Fe–N_p bonds. The two different relative imidazole orientations apparently result from the effects of crystal packing and the replacement of no more than $^1/_4$ of the axial ligands by an impurity imidazole. Analysis of the EPR data for the perpendicular species suggests that the approximate eclipsing of imidazole planes with porphyrin nitrogen axes leads to a much smaller derived rhombicity (V/Δ) compared to the complex with imidazole planes bisecting the porphyrin nitrogen axes (which was the case for [Fe(TPP)(2-MeHIm)₂]⁺, *J. Am. Chem. Soc.* **1986**, *108*, 5288). The average equatorial Fe–N_p bond distance is 1.978 (6) Å while the axial distances are 1.968 (4) and 1.976 (4) Å. The porphinato core has a modest D_{2d} ruffled conformation. Crystal data for [Fe(T2,6Cl₂PP)(1-VinIm)₂]ClO₄: $a = 12.288$ (4) Å, $b = 21.402$ (8) Å, $c = 20.975$ (6) Å, $\beta = 105.42$ (2)°, monoclinic, space group $P2_1/n$, $V = 5317.8$ Å³, $Z = 4$, 6642 observed data, $R_1 = 0.061$, $R_2 = 0.073$.

Introduction

Recent work by this research team has focused on the importance of the orientation of planar axial ligands in iron(III) porphyrinates on the electronic structure and magnetic properties of the iron atom. We have shown[4–8] that in some cases the effect of axial ligand orientation can be profound. To define the axial orientation, we must consider both its relationship to a defined Fe–N_p axis and when two planar axial ligands are present, their relationship to each other. The axial ligand orientation is given by the projection of the planar ligand onto the porphinato core; the orientation angle is defined by how close the projected plane falls on a Fe–N_p vector. For a given ligand plane projection, this angle can take on values between 0 and 45°. When there are two ligands, the two ligand planes define a relative orientation; the limiting cases are parallel (coplanar) and perpendicular relative orientations.

For one derivative, [Fe(OEP)(3-Cl-py)₂]ClO₄,[4] all three possible spin states have been observed in different crystalline forms;[5–7] control of the iron spin state appears to be regulated by and/or related to the absolute values of ligand orientation. With pyridine ligands, an orientation in which the ligand plane projections onto the porphinato core make small angles with an iron–porphyrin nitrogen vector yields an admixed intermediate-spin state; a rotation of ∼40° is required to achieve a low-spin state. The

high-spin state of this molecule is seen as the excited state of a thermal spin equilibrium system and thus has the same axial ligand orientation as the low-spin state. All three known different crystalline derivatives of [Fe(OEP)(3-Cl-py)₂]ClO₄ have effectively parallel relative orientations. In subsequent studies, we[8] and others[9] have also shown that the electron paramagnetic resonance (EPR) spectra of the bis-complexed low-spin derivatives are sensitive to axial ligand orientation. The *relative* orientation defines the nature of the EPR spectrum with parallel or approximately parallel orientations giving the well-known low-spin rhombic EPR spectrum. We have shown that the perpendicular orientation leads to an unusual EPR spectrum that we call "large g_{max}",[10] which consists of a single observed line (at very low temperatures) with a relatively large g value (g > 3.3). We have noted that such large g_{max} species might play a significant role[8] in modulating the reduction potentials of bis(histidine) coordinated-electron-transfer heme proteins.

The cytochromes b of complex III of mitochondria are known to have large g_{max} EPR spectra in their native forms,[11–13] but upon denaturation of the protein, the EPR spectra change to those of the normal rhombic B hemichrome type[11] and the reduction potentials drop by nearly 100 mV.[12] Widger and co-workers[14–16] have presented compelling evidence that the axial ligands of the mitochondrial and chloroplast cytochromes b are all histidines. It thus seems reasonable that this process of denaturation, which

(1) University of Notre Dame.
(2) Nagoya City University. Visiting Scholar at University of Notre Dame, Summer 1988.
(3) San Francisco State University. Present address: Department of Chemistry, University of Arizona, Tucson, AZ 85721.
(4) Abbreviations used include the following: 1-VinIm, 1-vinylimidazole; 3-Cl-py, 3-chloropyridine; 2-MeHIm, 2-methylimidazole; HIm, imidazole; RIm, N-substituted imidazole; c-MU and t-MU, *cis*- and *trans*-methyl urocanate (methyl 4-imidazoleacrylate), respectively; OEP, dianion of octaethylporphyrin; TPP, dianion of *meso*-tetraphenylporphyrin; T2,6Cl₂PP, dianion of *meso*-tetrakis(2,6-dichlorophenyl)-porphyrin; Proto IX, dianion of protoporphyrin IX; N_p porphinato nitrogen.
(5) Scheidt, W. R.; Geiger, D. K.; Haller, K. J. *J. Am. Chem. Soc.* **1982**, *104*, 495–9.
(6) Scheidt, W. R.; Geiger, D. K.; Hayes, R. G.; Lang, G. *J. Am. Chem. Soc.* **1983**, *105*, 2625–32.
(7) Scheidt, W. R.; Geiger, D. K.; Lee, Y. J.; Reed, C. A.; Lang, G. *Inorg. Chem.* **1987**, *26*, 1039–45.
(8) Walker, F. A.; Huynh, B. H.; Scheidt, W. R.; Osvath, S. R. *J. Am. Chem. Soc.* **1986**, *108*, 5288–97.

(9) Inniss, D.; Soltis, M.; Strouse, C. E. *J. Am. Chem. Soc.* **1988**, *110*, 5644–50.
(10) This EPR spectral feature has also been termed "HALS" (highly anisotropic low-spin) and "strong g_{max}". Both terminologies are somewhat misleading as greater anisotropy in the g tensor normally leads to a smaller calculated rhombicity V/Δ (complex is less rhombic, more tetragonal); moreover, the observed intensity of this spectral feature is very temperature dependent, and in general, the amplitude, in derivative mode, of the one observed feature is no greater than that of any one rhombic EPR signal feature at the same temperature.
(11) Salerno, J. C. *FEBS Lett.* **1983**, *162*, 257–61.
(12) Leigh, J. S.; Erecinska, M. *Biochim. Biophys. Acta* **1975**, *387*, 95–106.
(13) Erecinska, M.; Oshino, R.; Oshino, N.; Chance, B. *Arch. Biochem. Biophys.* **1973**, *157*, 431–45.
(14) Cramer, W. A.; Widger, W. R.; Hermann, R. G.; Trebst, A. *Proc. Natl. Acad. U.S.A.* **1984**, *81*, 674–8.
(15) Cramer, W. A.; Widger, W. R.; Hermann, R. G.; Trebst, A. *TIBS* **1985**, 125–129.
(16) Babcock, G. T.; Widger, W. R.; Cramer, W. A.; Oertling, W. A.; Metz, J. B. *Biochemistry* **1985**, *24*, 3638–3645.

leads concomitantly to a lowering of the reduction potential,[16] also leads to a "relaxation" of structure from the higher-energy perpendicular orientation to the lower-energy parallel orientation of axial imidazoles.

In our previous combined study of the EPR, Mössbauer, and X-ray crystallography of bisimidazole-coordinated iron(III) porphyrinates,[8] we were able to characterize three of the four limiting geometries possible for these systems: (1) axial ligands in parallel planes lying nearly over an Fe–N_p bond, or (2) approximately bisecting adjacent Fe–N_p vectors and (3) axial ligands in perpendicular planes bisecting adjacent Fe–N_p vectors. We commented at that time that the fourth possibility, in which the axial ligands were in perpendicular planes lying over Fe–N_p vectors, would be difficult to achieve in model complexes but might be quite likely to occur in natural systems where protein contacts and hydrogen-bonding frameworks could encourage sterically nonhindered histidine ligands to attain the seemingly desired (based on known structures of nonhindered imidazole complexes in which the ligands are in parallel planes) situation of eclipsing Fe–N_p bonds while yet having the two histidines in perpendicular planes. We have therefore sought model systems that might, for some reason, exhibit this fourth limiting ligand orientation.

In this paper, we report our initial observations on controlling the axial ligand orientation in iron(III) derivatives by using a "hindered" porphyrin derivative, tetrakis(2,6-dichlorophenyl)-porphyrin, an ortho-octasubstituted tetraarylporphyrin. We thought that such ortho substituents might restrict rotation about the axial ligand Fe–N bonds and hence lead to some orientational control. One of the compounds for which we initially obtained crystals displayed both normal rhombic and large g_{max} EPR signals. This species was obtained by the reaction of [Fe(T2,6Cl₂PP)-(OClO₃)] with 1-vinylimidazole. The molecular structure has been analyzed by single-crystal X-ray diffraction. The solid-state molecule is shown to have two different relative ligand orientations, one of which is the elusive perpendicular/eclipsed orientation.

Experimental Section

General Information. All solvents were distilled under argon prior to use. THF was distilled from sodium benzophenone ketyl while dichloromethane, chloroform, and hexane were distilled from CaH₂. 1-Vinylimidazole was obtained from Aldrich and used without further purification. Tetrakis(2,6-dichlorophenyl)porphyrin was initially prepared by appropriate modifications of the procedures used by Hatano for *meso*-tetrakis(2-cyanophenyl)porphyrin[17] and was obtained in 2.8% yield. The porphyrin was subsequently prepared by modification of the tetramesitylporphyrin preparation of Lindsey et al.[18,19] A 2-L three-necked flask, fitted with a condenser, argon inlet, and outlet was filled with 1.0 L of CHCl₃, 2,6-dichlorobenzaldehyde (2.33 g, 13.3 mmol), and freshly distilled pyrrole (0.93 mL, 13.4 mmol). The solution was purged with argon for 15 min, 2.2 mL of BF₃·OEt₂ (freshly opened bottle, Aldrich) was added, and the reaction mixture was stirred for 90 min at room temperature under a slow stream of argon. *p*-Chloranil (3.20 g, 13.0 mmol) was added, and the reaction mixture was gently refluxed (48 °C) for 1 h. The solution was evaporated to dryness, and methanol (≈800 mL) was added. A purple precipitate formed when the mixture was allowed to stand for 32 h. The precipitate was filtered and washed with methanol. The solid material was then dissolved in CHCl₃ and purified by silica gel chromatography with toluene as eluant. The sample was recrystallized from CH₂Cl₂/hexane. (Yield: 0.410 g, 13.8%.) [Fe(T2,6Cl₂PP)(OClO₃)] was prepared by the methanol of Dolphin et al.[20] EPR spectra were obtained at 77 and 7 K on a Varian E-12 EPR spectrometer operating at X-band frequency and equipped with Varian flowing-nitrogen and Air Products helium variable-temperature controllers, respectively. UV–vis spectra were recorded on Perkin-Elmer Lambda 4C or Shimadzu UV-2100 spectrometers, and IR spectra, on a Perkin-Elmer 883 spectrometer. Mass spectral analysis of 1-vinylimidazole was carried out on a Finnegan MAT 8930 mass spectrometer

(17) Hatano, K.; Anzai, K.; Kubo, T.; Tamai, S. *Bull. Chem. Soc. Jpn.* **1981**, *54*, 3518–21.

(18) Wagner, R. W.; Lawrence, D. S.; Lindsey, J. S. *Tetrahedron Lett.* **1987**, *28*, 3069–70.

(19) Lindsey has recently reported a procedure that yields the desired free base porphyrin in 24% yield: Lindsey, J. S.; Wagner, R. W. *J. Org. Chem.* **1989**, *54*, 828–36.

(20) Dolphin, D. H.; Sams, J. R.; Tsin, T. B. *Inorg. Chem.* **1977**, *16*, 711–3.

Table I. Crystal Data for [Fe(T2,6Cl₂PP)(1-VinIm)₂]ClO₄

formula	FeCl₉O₄N₈C₅₄H₃₂	V, Å³	5317.83
fw	1231.8	Z	4
space group	$P2_1/n$	no. of obsd data	6642
T, K	125	D(obsd), g/cm³	1.52[a]
a, Å	12.288 (4)	D(calcd), g/cm³	1.55[a]
b, Å	21.402 (8)	R_1	0.061
c, Å	20.975 (6)	R_2	0.073
β, deg	105.42 (2)		

[a] D(obsd) obtained at 298 K and D(calcd) at 125 K.

equipped with a Varian 3400 gas chromatograph and a 60-m Rtx-35 capillary column.

Stability Constant Measurements. The reaction of [Fe(T2,6Cl₂PP)-(OClO₃)] with 1-methylimidazole, 2-methylimidazole, and 1-vinylimidazole was monitored by following the spectral changes of ∼1 × 10⁻⁴ M solutions (CH₂Cl₂) of [Fe(T2,6Cl₂PP)(OClO₃)] upon addition of aliquots of ligand stock solution. The solutions were maintained at 24 ± 1 °C.

Syntheses of [Fe(T2,6Cl₂PP)(1-VinIm)₂]ClO₄. [Fe(T2,6Cl₂PP)(1-VinIm)₂]ClO₄ was prepared by dissolving [Fe(T2,6Cl₂PP)(OClO₃)] (50 mg, 0.048 mmol) and 1-vinylimidazole (45 mg, 0.480 mmol) in 20 mL of CH₂Cl₂. The reaction mixture was briefly stirred, and the solution was filtered and then layered with hexane for crystallization. Suitable crystals formed after 4 days.

Structure Determination of [Fe(T2,6Cl₂PP)(1-VinIm)₂]ClO₄. Preliminary examination of a crystal of [Fe(T2,6Cl₂PP)(1-VinIm)₂]ClO₄ on an Enraf-Nonius CAD4 diffractometer equipped with a locally modified Syntex LT-1 low-temperature attachment led to the assignment of a four-molecule primitive monoclinic unit cell, space group $P2_1/n$. Least-squares refinement based on 25 centered reflections gave the cell constants reported in Table I. Intensity data for [Fe(T2,6Cl₂PP)(1-VinIm)₂]ClO₄ were measured as described in Table SI. Four standard reflections were monitored during data collection. Intensity data were reduced with the suite of programs by Blessing.[21] All data with $F_o ≥ 3.0\sigma(F_o)$ were retained as observed and used in all subsequent least-squares refinement. The structure was solved with the direct methods program MULTAN.[22] Subsequent difference Fourier syntheses led to the location of remaining atoms. After several cycles of full-matrix least-squares refinement, a difference Fourier map suggested that there are two orientations of *one* of the 1-vinylimidazole ligands. For this ligand, all atoms of one orientation were well-defined while the other had only the five-atom imidazole ring well-defined. For this orientation, the imidazole side chain was quite diffuse with a number of possible atomic positions apparent in the difference Fourier synthesis. Consistent with the mass spectrum of the neat ligand, which revealed a small impurity having a molecular mass of 14 units higher than 1-vinylimidazole, this side chain was interpreted as a three-carbon group that was disordered over two different orientations. The difference Fourier synthesis also suggested locations of all hydrogen atoms in the structure except for those of the disordered imidazole ring. These hydrogen positions were idealized and included in subsequent cycles of least-squares refinement as fixed contributors (C–H = 0.95 Å, B(H) = 1.3 × B(C) Å²). Refinement was then carried to convergence with anisotropic thermal parameters for all atoms except two carbons, C(32) and C(42), of the disordered vinylimidazole rings and the two sets of propenyl carbon atoms. The final difference Fourier shows a 1.2 e/Å³ peak near the disordered propenyl chain; the map was otherwise judged featureless. Final atomic coordinates are listed in Table II. Final anisotropic temperature factors and hydrogen atom positions are given in Tables SII and SIII of the supplementary material.

Results

The results of the spectrophotometric titration of [Fe(T2,6Cl₂PP)(OClO₃)] with 1-vinylimidazole are shown in Figure

(21) Blessing, R. H. *Cryst. Rev.* **1987**, *1*, 3–58.

(22) Programs used in this study included local modifications of Main, Hull, Lessinger, Germain, Declerq, and Woolfson's MULTAN, Jacobson's ALLS, Zalkin's FORDAP, Busing and Levy's ORFFE, and Johnson's ORTEP2 Atomic form factors were from: Cromer, D. T.; Mann, J. B. *Acta Crystallogr., Sect. A* **1968**, *A24*, 321–3. Real and imaginary corrections for anomalous dispersion in the form factor of the iron atom were from: Cromer, D. T.; Liberman, D. J. *J. Chem. Phys.* **1970**, *53*, 1891–98. Scattering factors for hydrogen were from: Stewart, R. F.; Davidson, E. R.; Simpson, W. T. *Ibid.* **1965**, *42*, 3175–87.
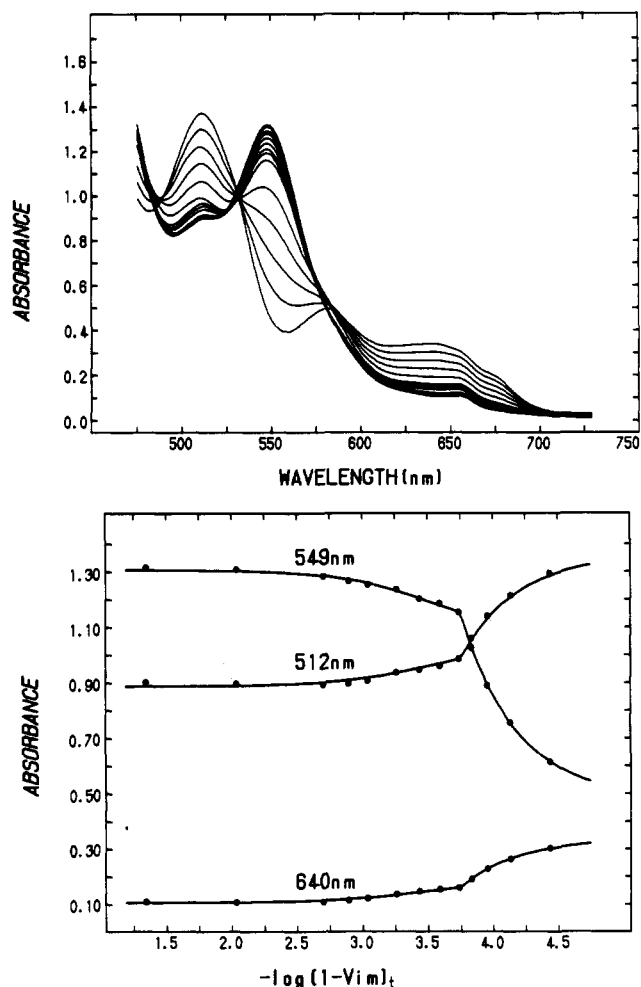
Figure 1. (a) Top: Spectrophotometric titration of [Fe(T2,6Cl₂PP)-(OClO₃)] with 1-vinylimidazole. Initial concentration of the porphyrin complex is 1.8×10^{-4} M and imidazole concentrations ranged from 0 to 4.5×10^{-2} M (CH₂Cl₂ solution). (b) Bottom: Diagram illustrating the least-squares fit of K'_1 and K_2 from the spectrophotometric data at 640, 512, and 549 nm.

1a. The spectral data yield values for ligand binding constants K'_1 and K_2 where

$$K'_1 = \frac{[\text{FePL}^+][\text{ClO}_4^-]}{[\text{FePOClO}_3][\text{L}]}$$

and

$$K_2 = \frac{[\text{FePL}_2^+]}{[\text{FePL}^+][\text{L}]}$$

The analysis of the spectral changes at low ligand concentrations, especially near the region where ligand concentration is equal to that of the starting complex, was most consistent with the intermediate species being dissociated ions; i.e., the intermediate is the five-coordinate [Fe(P)(L)]⁺ complex with perchlorate not bonded or tightly ion paired. Least-squares fits of the spectral data at three different wavelengths are shown in Figure 1b. The resulting values of K'_1 and K_2 and derived values of β'_2 for 1-vinyl-, 1-methyl-, and 2-methylimidazole ligands are given in Table III.

In our hands, crystallization of [Fe(T2,6Cl₂PP)(OClO₃)] and 1-vinylimidazole apparently yields two different crystalline materials. In addition to well-formed X-ray quality crystals, we also obtained a microcrystalline material. The EPR spectra of the two crystalline materials were found to differ. The EPR spectrum of the X-ray quality crystals has both large g_{max} and "normal" rhombic signals as shown in Figure 2. The rhombic component has $g_z = 2.90$, $g_y = 2.27$, and $g_x = 1.57$ while the large g_{max} EPR component has a peak at $g_z = 3.70$. The microcrystalline material exhibits only a normal rhombic EPR spectrum with $g_z = 2.88$,
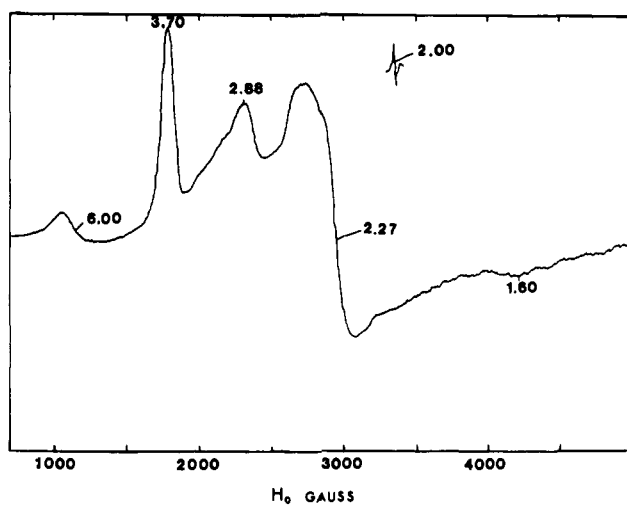

Figure 2. EPR spectrum of crystals of [Fe(T2,6Cl₂PP)(1-VinIm)₂]ClO₄ from the same batch as that for which the structure was determined, recorded at 7 K.
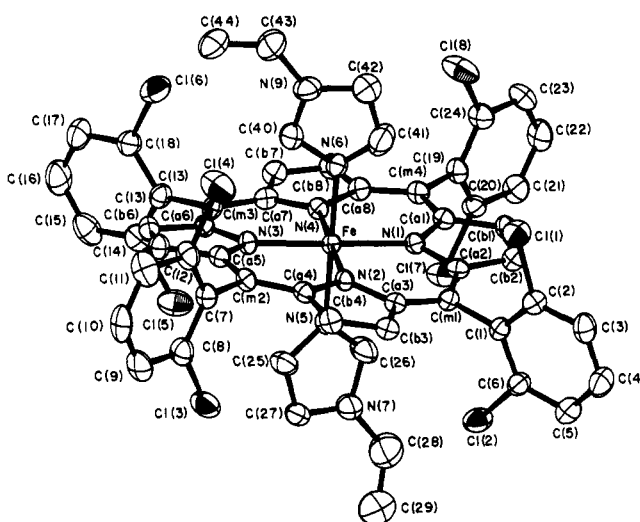
Figure 3. ORTEP diagram of the [Fe(T2,6Cl₂PP)(1-VinIm)₂]ClO₄ molecule showing the two axial ligands that are nearly parallel to each other. The atom labels of the molecule are displayed.

$g_y = 2.27$, and $g_x = 1.60$. The frozen-solution EPR of the complex consists of only a normal rhombic spectrum with $g_z = 2.88$, $g_y = 2.30$, and $g_x = 1.57$. (All EPR measurements at 7 K.) The rhombic EPR parameters allow calculation of the "tetragonality" (Δ/λ) and "rhombicity" (V/Δ) parameters of Blumberg and Peisach[23] for the three samples: 3.44, 0.58; 3.57, 0.58; and 3.26, 0.63, respectively.

Consistent with the growth of the two different types of crystals with different EPR spectra, mass spectral analysis of the vinylimidazole sample used as the ligand in the crystallization procedures showed the presence of a small amount of an impurity having a molecular mass 14 mass units higher than that of 1-vinylimidazole. While the additional CH₂ unit could in principle be bound to one of the ring carbon atoms of the imidazole, X-ray crystallographic analysis (vide infra) suggests that this extra CH₂ unit is part of the nitrogen substituent, i.e., 1-propenylimidazole, where the position of the double bond is not known. Most importantly, the presence of a small amount of an impurity of 1-propenylimidazole in the sample of 1-vinylimidazole from which the crystalline sample was synthesized is truly demonstrated. As was mentioned in the Experimental Section and will be discussed below, it appears that this small amount of impurity was concentrated by several orders of magnitude during the crystallization

(23) Blumberg, W. E.; Peisach, J. *Adv. Chem. Ser.* **1971**, *100*, 271–91.

Table II. Fractional Coordinates for [Fe(T2,6Cl$_2$PP)(1-VinIm)$_2$]ClO$_4$[a]

atom	x	y	z	atom	x	y	z
Fe	0.12360 (5)	0.23314 (3)	0.60740 (3)	C(14)	0.0381 (5)	0.10167 (29)	0.82542 (27)
N(1)	0.2526 (3)	0.28437 (19)	0.59927 (19)	C(15)	0.0120 (5)	0.0610 (4)	0.8712 (3)
N(2)	0.0242 (3)	0.27679 (19)	0.52992 (19)	C(16)	0.0108 (6)	−0.0020 (4)	0.8591 (4)
N(3)	−0.0047 (3)	0.18080 (20)	0.61473 (19)	C(17)	0.0385 (6)	−0.0259 (3)	0.8050 (4)
N(4)	0.2227 (3)	0.19066 (19)	0.68538 (19)	C(18)	0.0633 (5)	0.01513 (28)	0.76000 (29)
N(5)	0.0829 (3)	0.29723 (20)	0.66430 (20)	C(19)	0.5287 (4)	0.24116 (26)	0.72029 (25)
N(6)	0.1602 (4)	0.16955 (20)	0.54805 (21)	C(20)	0.5712 (4)	0.28101 (24)	0.77366 (27)
N(7)	0.0833 (5)	0.38448 (27)	0.7207 (3)	C(21)	0.6871 (4)	0.2898 (3)	0.8007 (3)
N(8)	0.2493 (10)	0.0882 (5)	0.5165 (6)	C(22)	0.7609 (4)	0.2581 (3)	0.7742 (3)
N(9)	0.1362 (9)	0.0857 (5)	0.4854 (6)	C(23)	0.7235 (5)	0.2157 (3)	0.72356 (29)
C(a1)	0.3640 (4)	0.27867 (23)	0.63414 (23)	C(24)	0.6070 (4)	0.20836 (28)	0.69648 (27)
C(a2)	0.2506 (4)	0.33435 (23)	0.55719 (23)	C(25)	−0.0216 (5)	0.30753 (29)	0.6740 (3)
C(a3)	0.0494 (4)	0.32934 (22)	0.49866 (22)	C(26)	0.1455 (5)	0.3444 (3)	0.6945 (4)
C(a4)	−0.0874 (4)	0.26356 (25)	0.49840 (23)	C(27)	−0.0204 (5)	0.35952 (27)	0.71007 (29)
C(a5)	−0.1117 (4)	0.17746 (24)	0.57063 (23)	C(28)	0.1178 (9)	0.4450 (5)	0.7438 (5)
C(a6)	−0.0068 (4)	0.13745 (23)	0.66345 (24)	C(29)	0.0550 (11)	0.4894 (5)	0.7604 (8)
C(a7)	0.1907 (4)	0.14835 (24)	0.72637 (24)	C(30)	0.2404 (11)	0.1227 (7)	0.5688 (6)
C(a8)	0.3381 (4)	0.19802 (24)	0.71132 (24)	C(31)	0.1230 (12)	0.1613 (6)	0.4813 (5)
C(b1)	0.4331 (4)	0.32485 (25)	0.61255 (25)	C(32)	0.1732 (13)	0.1139 (6)	0.4596 (6)
C(b2)	0.3617 (4)	0.35921 (25)	0.56499 (26)	C(33)	0.3235 (29)	0.0309 (18)	0.5298 (25)
C(b3)	−0.0464 (4)	0.34889 (24)	0.44684 (24)	C(34)	0.3898 (23)	−0.0026 (13)	0.5002 (13)
C(b4)	−0.1304 (4)	0.30742 (26)	0.44584 (24)	C(35)	0.427 (4)	−0.0056 (24)	0.4513 (24)
C(b5)	−0.1784 (4)	0.13087 (25)	0.59218 (25)	C(33)′	0.3218 (10)	0.0361 (12)	0.5128 (9)
C(b6)	−0.1151 (4)	0.10684 (26)	0.64985 (26)	C(34)′	0.4089 (12)	0.0229 (15)	0.5685 (10)
C(b7)	0.2875 (4)	0.12911 (25)	0.77870 (25)	C(35)′	0.487 (4)	0.0075 (24)	0.5495 (24)
C(b8)	0.3781 (4)	0.15913 (26)	0.76880 (25)	C(40)	0.1057 (10)	0.1159 (6)	0.5338 (6)
C(m1)	0.1543 (4)	0.35830 (23)	0.51234 (24)	C(41)	0.2167 (17)	0.1758 (7)	0.5025 (8)
C(m2)	−0.1507 (4)	0.21638 (23)	0.51620 (23)	C(42)	0.2145 (16)	0.1224 (7)	0.4676 (8)
C(m3)	0.0831 (4)	0.12407 (23)	0.71758 (24)	C(43)	0.1009 (14)	0.0253 (7)	0.4604 (9)
C(m4)	0.4058 (4)	0.23772 (24)	0.68705 (23)	C(44)	0.0300 (14)	−0.0114 (7)	0.4829 (8)
C(1)	0.1689 (4)	0.41645 (23)	0.47707 (25)	Cl(1)	0.20176 (14)	0.34545 (7)	0.37763 (7)
C(2)	0.1923 (5)	0.41636 (26)	0.41531 (26)	Cl(2)	0.13738 (14)	0.47972 (7)	0.58308 (7)
C(3)	0.2124 (5)	0.4711 (3)	0.38427 (29)	Cl(3)	−0.31858 (12)	0.30043 (8)	0.55636 (9)
C(4)	0.2080 (6)	0.5275 (3)	0.4146 (4)	Cl(4)	−0.20502 (14)	0.12035 (10)	0.40542 (10)
C(5)	0.1856 (5)	0.53059 (28)	0.4759 (3)	Cl(5)	0.03936 (14)	0.18161 (8)	0.83964 (8)
C(6)	0.1664 (4)	0.47539 (25)	0.50635 (27)	Cl(6)	0.09559 (19)	−0.01416 (8)	0.68960 (10)
C(7)	−0.2720 (4)	0.20817 (25)	0.47950 (24)	Cl(7)	0.47741 (12)	0.32140 (7)	0.80794 (8)
C(8)	−0.3572 (4)	0.24188 (29)	0.49738 (29)	Cl(8)	0.55869 (13)	0.15683 (10)	0.63139 (9)
C(9)	−0.4713 (4)	0.2295 (3)	0.4700 (3)	Cl(9)	0.25995 (17)	0.04776 (9)	0.28587 (10)
C(10)	−0.5010 (5)	0.1827 (3)	0.4228 (3)	O(1)	0.2813 (6)	−0.01733 (29)	0.2781 (4)
C(11)	−0.4207 (5)	0.1496 (4)	0.4025 (3)	O(2)	0.1704 (6)	0.0528 (3)	0.31796 (29)
C(12)	−0.3071 (5)	0.16259 (29)	0.43058 (28)	O(3)	0.3561 (6)	0.0801 (4)	0.3259 (5)
C(13)	0.0626 (4)	0.08016 (25)	0.76823 (26)	O(4)	0.2308 (6)	0.0779 (3)	0.2221 (3)

[a] The estimated standard deviations of the least significant digits are given in parentheses.

Table III. Equilibrium Constants for Binding of 1-Vinylimidazole, 1-Methylimidazole, and 2-Methylimidazole to [Fe(T2,6-Cl$_2$PP)OClO$_3$]

ligand	K'_1	K_2, M^{-1}	$\beta'_2 = K'_1 K_2$, M^{-1}
1-vinylimidazole	7500	3450	2.59 × 10^7
1-methylimidazole	10	14000	1.40 × 10^5
2-methylimidazole	620	21000	1.30 × 10^7

process into the large crystals used for the X-ray analysis, to the point where it accounts for up to one-fourth of the axial ligand present in these crystals. For simplicity, however, we will continue to refer to the complex as [Fe(T2,6Cl$_2$PP)(1-VinIm)$_2$]ClO$_4$.

The molecular structure of [Fe(T2,6Cl$_2$PP)(1-VinIm)$_2$]ClO$_4$ consists of one independent molecule in the asymmetric unit. The crystal used for the structure determination was typical of those that exhibited both rhombic and large g$_{max}$ EPR signals. However, apparent disorder in the crystal structure results from molecules of [Fe(T2,6Cl$_2$PP)(1-VinIm)$_2$]ClO$_4$ that have different relative orientation of axial imidazole ligands. A view of one of the two axial ligand orientations is shown in Figure 3 along with the atom numbering scheme. Individual values of bond distances and angles are given in Tables IV and V, respectively. Averaged values for the chemically equivalent bond distances and angles are shown in Figure 4. The average Fe to porphyrin nitrogen bond distance is 1.978 (8) Å. The average axial Fe–N bond distance is 1.972 (6) Å. Figure 4 is a formal diagram showing the deviations of the atoms from the mean plane of the 24-atom porphinato core (in units of 0.01 Å).
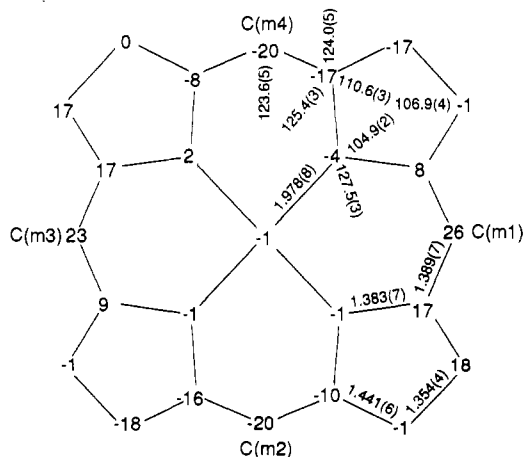

Figure 4. Formal diagram of the porphinato core in the [Fe-(T2,6Cl$_2$PP)(1-VinIm$_2$]ClO$_4$ molecule displaying the averaged values of bond distances and angles in the core. Numbers in parentheses are the root-mean-square deviations from the averaged values. Deviation of each unique atom from the mean plane of the core (in units of 0.01 Å) are shown.

Discussion

Metal complexes of tetrakis(2,6-disubstituted phenyl)porphyrins have found considerable utility in the investigation of the hydroxylation reactions that attempt to model those of cytochrome

Table IV. Bond Distances in [Fe(T2,6Cl₂PP)(1-VinIm)₂]ClO₄ᵃ

Fe–N(1)	1.971 (4)	C(6)–C(1)	1.408 (7)
Fe–N(2)	1.988 (4)	C(6)–Cl(2)	1.741 (6)
Fe–N(3)	1.973 (4)	C(7)–C(8)	1.402 (8)
Fe–N(4)	1.981 (4)	C(8)–C(9)	1.393 (8)
Fe–N(5)	1.968 (4)	C(8)–Cl(3)	1.736 (6)
Fe–N(6)	1.976 (4)	C(9)–C(10)	1.385 (10)
N(1)–C(a1)	1.375 (6)	C(10)–C(11)	1.372 (10)
N(1)–C(a2)	1.383 (6)	C(11)–C(12)	1.391 (8)
N(2)–C(a3)	1.378 (6)	C(12)–C(7)	1.398 (8)
N(2)–C(a4)	1.384 (6)	C(12)–Cl(4)	1.738 (6)
N(3)–C(a5)	1.394 (6)	C(13)–C(14)	1.391 (8)
N(3)–C(a6)	1.386 (6)	C(14)–C(15)	1.395 (9)
N(4)–C(a7)	1.376 (7)	C(14)–Cl(5)	1.736 (6)
N(4)–C(a8)	1.386 (6)	C(15)–C(16)	1.371 (12)
N(5)–C(25)	1.370 (7)	C(16)–C(17)	1.368 (12)
N(5)–C(26)	1.324 (8)	C(17)–C(18)	1.383 (8)
N(6)–C(30)	1.392 (13)	C(18)–C(13)	1.403 (8)
N(6)–C(31)	1.365 (12)	C(18)–Cl(6)	1.744 (6)
N(6)–C(40)	1.322 (13)	C(19)–C(20)	1.394 (8)
N(6)–C(41)	1.328 (15)	C(20)–C(21)	1.398 (7)
C(a1)–C(b1)	1.452 (7)	C(20)–Cl(7)	1.742 (5)
C(a1)–C(m4)	1.400 (7)	C(21)–C(22)	1.364 (9)
C(a2)–C(b2)	1.433 (7)	C(22)–C(23)	1.379 (9)
C(a2)–C(m1)	1.399 (7)	C(23)–C(24)	1.402 (7)
C(a3)–C(b3)	1.436 (6)	C(24)–C(19)	1.402 (7)
C(a3)–C(m1)	1.389 (7)	C(24)–Cl(8)	1.733 (6)
C(a4)–C(b4)	1.438 (7)	C(25)–C(27)	1.384 (8)
C(a4)–C(m2)	1.385 (7)	C(27)–N(7)	1.345 (8)
C(a5)–C(b5)	1.438 (7)	N(7)–C(26)	1.359 (8)
C(a5)–C(m2)	1.391 (7)	N(7)–C(28)	1.408 (11)
C(a6)–C(b6)	1.443 (7)	C(28)–C(29)	1.327 (15)
C(a6)–C(m3)	1.387 (7)	C(31)–C(32)	1.329 (7)
C(a7)–C(b7)	1.447 (7)	C(32)–N(8)	1.417 (7)
C(a7)–C(m3)	1.386 (7)	N(8)–C(30)	1.351 (7)
C(a8)–C(b8)	1.440 (7)	N(8)–C(33)	1.509 (38)
C(a8)–C(m4)	1.378 (7)	N(8)–C(33)′	1.443 (10)
C(b1)–C(b2)	1.357 (7)	C(33)–C(34)	1.354 (46)
C(b3)–C(b4)	1.358 (7)	C(34)–C(35)	1.179 (5)
C(b5)–C(b6)	1.353 (8)	N(33)′–C(34)′	1.387 (5)
C(b7)–C(b8)	1.349 (7)	C(34)′–C(35)′	1.233 (55)
C(m1)–C(1)	1.483 (7)	C(41)–C(42)	1.354 (22)
C(m2)–C(7)	1.495 (6)	C(42)–N(9)	1.370 (20)
C(m3)–C(13)	1.489 (7)	N(9)–C(40)	1.339 (16)
C(m4)–C(19)	1.487 (6)	N(9)–C(43)	1.418 (17)
C(1)–C(2)	1.399 (7)	C(43)–C(44)	1.349 (23)
C(2)–C(3)	1.394 (8)	Cl(9)–O(1)	1.435 (6)
C(2)–Cl(1)	1.729 (6)	Cl(9)–O(2)	1.438 (6)
C(3)–C(4)	1.372 (10)	Cl(9)–O(3)	1.433 (7)
C(4)–C(5)	1.386 (10)	Cl(9)–O(4)	1.441 (7)
C(5)–C(6)	1.393 (8)		

ᵃThe estimated standard deviations of the least significant digits are given in parentheses. Primed and unprimed symbols denote the two disordered propenyl side chain positions.

P-450.[24–33] Two major types of ortho substituents have been utilized in these metallotetraphenylporphyrin derivatives: methyl

groups (as in tetramesitylporphyrin, H₂TMP) and halogen atoms (F, Cl, Br). The purpose of the phenyl ortho substituents has been 2-fold: (1) to protect the metal binding site by preventing the high-valent oxometal ion from intermolecular reactions that lead to PM–O–MP dimers,[33] and (2) to protect the porphyrin macrocycle from degradation by either intra- or intermolecular reactions with the high valent metal species.[24–32] Studies of the epoxidation of olefins by high-valent derivatives of [Fe-(T2,6X₂PP)(Cl)] have clearly shown that for both X = Cl and Br there is a large cis/trans selectivity,[26,32] suggesting that these ortho substituents are able to hinder the approach of the trans olefin to the ferryl oxygen. From this and other related findings, including the fact that certain of these phenyl ortho substituents also hinder the rotation of planar axial ligands such as 2-methylimidazole about the metal–ligand bond,[34] the popular notion has developed that these groups may hinder the binding of axial ligands to the metal. Contrary to this popular notion, the values of the binding constants found for the reaction of [Fe-(T2,6Cl₂PP)(OClO₃)] with 1-vinyl-, 1-methyl-, and 2-methyl-imidazole in methylene chloride (log β'_2 = 7.41, 5.16, and 7.12, respectively where $\beta'_2 = K'_1 K_2$) are larger than the values found by Walker et al. in methylene chloride,[35] chloroform,[35,36] and dimethylformamide[35] for the analogous reactions with [Fe(TP-P)Cl] and a series of substituted (tetraarylporphinato)iron(III) halides with a variety of imidazole ligands. However, most of the data are not directly comparable because in the present case the products are the dissociated ions rather than the tight ion pairs generally found in the earlier studies where chloride was the anion.[35,36] For reactions previously studied in dichloromethane, only the data for the reaction of [Fe(TPP)Cl] with 1-methyl-imidazole is comparable; in this case log β'_2 ≈ −0.3. It is reasonable to expect that the perchlorate ion would dissociate much more readily than chloride, since the negative charge is delocalized over the four oxygen atoms. However, it is surprising to find the difference in β'_2 for 1-methylimidazole to be nearly 6 orders of magnitude. In fact, if the *o*-chloro groups are acting as electron-withdrawing substituents, as do *m*- and *p*-chloro substituents,[35,36] then the difference is well over 6 orders of magnitude since formation of bis complexes of iron(III) porphyrinates is enhanced by *electron-donating* substituents.[35,36] The ortho substituents appear to behave differently; an investigation of the electronic properties of ortho substituents is in progress.[37] The difference in log β'_2 for L = 1-methylimidazole and 2-methyl-imidazole found in this study (log β'_2 = 5.16 and 7.12, respectively) as compared to the much smaller difference in log β_2 in the earlier study (log β_2 = 4.00 and 3.57, respectively[35]) is probably a complex combination of differences in the solvation of the separated ions as compared to the tight ion pairs for the N–R and N–H imidazoles in dichloromethane, as well as possible differences in the ability of the two porphyrins to accommodate the hindered 2-methylimidazole ligand by deformation of the porphyrin core. The more than 2 orders of magnitude difference in β'_2 for 1-methyl- and 1-vinylimidazole is not readily explicable in terms of steric or solvation effects and must therefore result from a difference in the σ and/or π basicity of the N(3) nitrogen of the two imidazoles. Further speculation on the differences in log β'_2 for 1-methyl- and 1-vinylimidazole in this study is probably unwarranted. It is clear, however, that the large values of log β'_2 for all three ligands of this study show that the steric bulk of the peripheral substituents certainly does not have a deleterious effect on the binding of imidazoles to iron(III). A complete systematic comparison of equilibrium constants with hindered porphyrin ligands is in progress and will be published elsewhere.[38]

(24) Traylor, P. S.; Dolphin, D.; Traylor, T. G. *J. Chem. Soc., Chem. Commun.* **1984**, 279–80. Traylor, T. G.; Tsuchiya, S. *Inorg. Chem.* **1987**, *26*, 1338–41. Traylor, T. G.; Tsuchiya, S. *Ibid.* **1988**, *27*, 4520. Traylor, T. G.; Xu, F. *J. Am. Chem. Soc.* **1988**, *110*, 1953–8. Traylor, T. G.; Nakano, T.; Miksztal, A. R.; Dunlap, B. E. *Ibid.* **1986**, *108*, 7861–2.
(25) Artaud, I.; Devocelle, L.; Battioni, J. P.; Girault, J.-P.; Mansuy, D. *J. Am. Chem. Soc.* **1987**, *109*, 3782–3.
(26) Traylor, T. G.; Miksztal, A. R. *J. Am. Chem. Soc.* **1987**, *109*, 2770–4.
(27) Groves, J. T.; Stern, M. K. *J. Am. Chem. Soc.* **1988**, *110*, 8628–38.
(28) Rodgers, K. R.; Goff, H. M. *J. Am. Chem. Soc.* **1988**, *110*, 7049–60.
(29) Sugimoto, H.; Tung, H.-C.; Sawyer, D. T. *J. Am. Chem. Soc.* **1988**, *110*, 2465–70.
(30) Gold, A.; Jayaraj, K.; Doppelt, P.; Weiss, R.; Chottard, G.; Bill, E.; Ding, Trautwein, A. X. *J. Am. Chem. Soc.* **1988**, *110*, 5756–61.
(31) Garrison, J. M.; Bruice, T. C. *J. Am. Chem. Soc.* **1989**, *111*, 191–8. Balasubramanian, P. N.; Lindsay Smith, J. R.; Davis, M. J.; Kaaret, T. W.; Bruice, T. C. *Ibid.* **1989**, *111*, 1477–83. Panicucci, R.; Bruice, T. C. *Ibid.* **1990**, *112*, 6063–71. Murata, K.; Panicucci, R.; Gopinath, E.; Bruice, T. C. *Ibid.* **1990**, *112*, 6072–83.
(32) Collman, J. P.; Hampton, P. D.; Brauman, J. I.; Panicucci, R.; Bruice, T. C. *J. Am. Chem. Soc.* **1990**, *112*, 2977–86, 2986–98.
(33) Cheng, R.-T.; Latos-Grazynski; Balch, A. L. *Inorg. Chem.* **1982**, *21*, 2412–8.

(34) Nakamura, M.; Groves, J. T. *Tetrahedron* **1988**, *44*, 3225–30.
(35) Walker, F. A.; Lo, M. W.; Ree, M. T. *J. Am. Chem. Soc.* **1976**, *98*, 5553–60.
(36) Balke, V. L.; Walker, F. A.; West, J. T. *J. Am. Chem. Soc.* **1985**, *107*, 1226–33.
(37) Walker, F. A.; Graul, R. C.; Tipton, A. R.; Norvell, C. J.; Seaman, D. H.; Koerner, R. Unpublished results.
(38) Hatano, K.; Uno, T.; Inoue, H.; Kato, K.; Scheidt, W. R. Preliminary account presented at the 109th Annual Meeting of the Pharmaceutical Society of Japan, Nagoya, Japan, 1989; Abstract 5P 10-1.

Table V. Bond Angles in [Fe(T2,6Cl$_2$PP)(1-VinIm)$_2$]ClO$_4$^{a}

N(1)FeN(2)	90.07 (16)	C(m1)C(1)C(2)	122.8 (4)	C(b2)C(a2)C(m1)	123.4 (5)	C(19)C(20)Cl(7)	119.1 (4)
N(1)FeN(3)	179.09 (17)	C(m1)C(1)C(6)	121.0 (4)	N(1)C(a2)C(m1)	125.5 (4)	C(21)C(20)Cl(7)	118.7 (4)
N(1)FeN(4)	89.70 (16)	C(2)C(1)C(6)	116.0 (3)	N(2)C(a3)C(b3)	110.8 (4)	C(20)C(21)C(22)	119.0 (5)
N(1)FeN(5)	90.27 (17)	C(1)C(2)C(3)	122.4 (5)	C(b3)C(a3)C(m1)	123.7 (4)	C(21)C(22)C(23)	121.3 (5)
N(1)FeN(6)	90.32 (17)	C(1)C(2)Cl(1)	118.6 (4)	N(2)C(a3)C(m1)	125.4 (4)	C(22)C(23)C(24)	118.7 (5)
N(2)FeN(3)	90.02 (16)	C(3)C(2)Cl(1)	118.9 (4)	N(2)C(a4)C(b4)	110.4 (4)	C(23)C(24)C(19)	121.9 (5)
N(2)FeN(4)	179.22 (17)	C(2)C(3)C(4)	119.3 (5)	C(b4)C(a4)C(m2)	124.4 (4)	C(23)C(24)Cl(8)	119.3 (4)
N(2)FeN(5)	88.18 (16)	C(3)C(4)C(5)	120.9 (6)	N(2)C(a4)C(m2)	125.2 (4)	C(19)C(24)Cl(8)	118.8 (4)
N(2)FeN(6)	90.11 (17)	C(4)C(5)C(6)	119.0 (6)	N(3)C(a5)C(b5)	110.1 (4)	N(5)C(25)C(27)	110.3 (5)
N(3)FeN(4)	90.21 (16)	C(5)C(6)C(1)	122.3 (5)	C(b5)C(a5)C(m2)	124.9 (4)	C(25)C(27)N(7)	106.9 (5)
N(3)FeN(5)	90.63 (17)	C(5)C(6)Cl(2)	118.7 (4)	N(3)C(a5)C(m2)	124.9 (4)	C(27)N(7)C(26)	107.0 (5)
N(3)FeN(6)	88.78 (17)	C(1)C(6)Cl(2)	119.0 (4)	N(3)C(a6)C(b6)	110.8 (4)	N(7)C(26)N(5)	110.9 (5)
N(4)FeN(5)	91.08 (17)	C(m2)C(7)C(8)	121.0 (4)	C(b6)C(a6)C(m3)	124.1 (4)	C(27)N(7)C(28)	127.4 (6)
N(4)FeN(6)	90.63 (17)	C(m2)C(7)C(12)	122.0 (4)	N(3)C(a6)C(m3)	125.1 (4)	C(26)N(7)C(28)	124.7 (6)
N(5)FeN(6)	178.20 (17)	C(8)C(7)C(12)	116.6 (3)	N(4)C(a7)C(b7)	110.3 (4)	N(7)C(28)C(29)	127.3 (9)
FeN(1)C(a1)	127.9 (3)	C(7)C(8)C(9)	122.2 (6)	C(b7)C(a7)C(m3)	123.8 (5)	N(6)C(31)C(32)	113.0 (10)
FeN(1)C(a2)	127.4 (3)	C(7)C(8)Cl(3)	118.7 (4)	N(4)C(a7)C(m3)	125.8 (4)	C(31)C(32)N(8)	105.6 (11)
C(a1)N(1)C(a2)	104.7 (4)	C(9)C(8)Cl(3)	119.1 (5)	N(4)C(a8)C(b8)	110.4 (4)	C(32)N(8)C(30)	107.2 (10)
FeN(2)C(a3)	127.3 (3)	C(8)C(9)C(10)	118.5 (6)	C(b8)C(a8)C(m4)	124.1 (4)	N(8)C(30)N(6)	110.0 (10)
FeN(2)C(a4)	127.6 (3)	C(9)C(10)C(11)	121.4 (5)	N(4)C(a8)C(m4)	125.5 (4)	C(32)N(8)C(33)	134.5 (20)
C(a3)N(2)C(a4)	105.0 (4)	C(10)C(11)C(12)	119.2 (6)	C(a1)C(b1)C(b2)	106.3 (4)	C(30)N(8)C(33)	118.0 (21)
FeN(3)C(a5)	127.6 (3)	C(11)C(12)C(7)	122.0 (6)	C(a2)C(b2)C(b1)	107.0 (4)	C(32)N(8)C(33)'	122.2 (9)
FeN(3)C(a6)	127.5 (3)	C(11)C(12)Cl(4)	119.4 (5)	C(a3)C(b3)C(b4)	106.8 (4)	C(30)N(8)C(33)'	130.6 (10)
C(a5)N(3)C(a6)	104.8 (4)	C(7)C(12)Cl(4)	118.6 (4)	C(a4)C(b4)C(b3)	107.0 (4)	N(8)C(33)C(34)	138.9 (42)
FeN(4)C(a7)	127.0 (3)	C(m3)C(13)C(14)	121.5 (4)	C(a5)C(b5)C(b6)	107.7 (4)	N(8)C(33)'C(34)'	117.5 (4)
FeN(4)C(a8)	127.7 (3)	C(m3)C(13)C(18)	121.9 (4)	C(a6)C(b6)C(b5)	106.6 (4)	C(33)C(34)C(35)	144.5 (40)
C(a7)N(4)C(a8)	105.2 (4)	C(14)C(13)C(18)	116.5 (4)	C(a7)C(b7)C(b8)	107.1 (4)	C(33)'C(34)'C(35)'	106.7 (24)
FeN(5)C(25)	127.0 (4)	C(13)C(14)C(15)	122.0 (6)	C(a8)C(b8)C(b7)	107.0 (4)	N(6)C(41)C(42)	111.5 (12)
FeN(5)C(26)	127.7 (4)	C(13)C(14)Cl(5)	118.7 (4)	C(a2)C(m1)C(a3)	123.2 (5)	C(41)C(42)N(9)	104.5 (13)
C(25)N(5)C(26)	104.8 (5)	C(15)C(14)Cl(5)	119.3 (5)	C(a2)C(m1)C(1)	116.7 (4)	C(42)N(9)C(40)	106.7 (10)
FeN(6)C(30)	124.0 (6)	C(14)C(15)C(16)	118.6 (6)	C(a3)C(m1)C(1)	120.0 (4)	N(9)C(40)N(6)	111.4 (10)
FeN(6)C(31)	131.8 (6)	C(15)C(16)C(17)	122.0 (6)	C(a4)C(m2)C(a5)	124.2 (4)	C(42)N(9)C(43)	126.1 (12)
C(30)N(6)C(31)	104.1 (8)	C(16)C(17)C(18)	118.5 (7)	C(a4)C(m2)C(7)	120.1 (4)	C(40)N(9)C(43)	127.0 (12)
FeN(6)C(40)	123.6 (6)	C(17)C(18)C(13)	122.5 (6)	C(a5)C(m2)C(7)	115.5 (4)	N(9)C(43)C(44)	124.3 (14)
FeN(6)C(41)	129.4 (7)	C(17)C(18)Cl(6)	119.4 (5)	C(a7)C(m3)C(a6)	123.7 (4)	O(1)Cl(1)O(2)	108.2 (4)
C(40)N(6)C(41)	104.7 (9)	C(13)C(18)Cl(6)	118.1 (4)	C(a6)C(m3)C(13)	117.7 (4)	O(1)Cl(1)O(3)	112.9 (5)
N(1)C(a1)C(b1)	110.8 (4)	C(m4)C(19)C(20)	121.6 (4)	C(a7)C(m3)C(13)	118.6 (4)	O(1)Cl(1)O(4)	109.7 (4)
C(b1)C(a1)C(m4)	123.4 (4)	C(m4)C(19)C(24)	121.5 (4)	C(a8)C(m4)C(a1)	123.2 (4)	O(2)Cl(1)O(3)	107.7 (5)
N(1)C(a1)C(m4)	125.5 (4)	C(20)C(19)C(24)	116.8 (3)	C(a8)C(m4)C(19)	119.6 (4)	O(2)Cl(1)O(4)	111.6 (4)
N(1)C(a2)C(b2)	111.1 (4)	C(19)C(20)C(21)	122.1 (5)	C(a1)C(m4)C(19)	117.0 (4)	O(3)Cl(1)O(4)	106.8 (5)

^{a} The estimated standard deviations of the least significant digits are given in parentheses. Primed and unprimed symbols denote the two disordered propenyl side chain positions.

The crystal structure determination of [Fe(T2,6Cl$_2$PP)(1-VinIm)$_2$]ClO$_4$ clearly showed that the complex is the expected bis(imidazole) species. The determination also revealed that one of the two axial imidazole ligands is disordered. The imidazole ligand on one side of the porphinato plane has two different orientations with the coordinating nitrogen atom (N(6)) as the only common atom. In addition, one set of these disordered imidazole ligands also has a disordered exo-nitrogen substituent. The carbon chain in this ligand contains an additional carbon atom; i.e., there is a three-carbon side chain instead of the expected vinyl group. Figure 5 is an ORTEP diagram of the molecule showing the relative orientations of all axial ligands. The planes of the two disordered imidazole ligands (the top pair of Figure 5) make a dihedral angle of 83°. The relative populations of the two orientations of the disordered ligand are approximately equal as deduced from a crystallographic population analysis. Moreover, subsequent analysis of crystal packing effects (vide infra) also suggests that the populations of the two orientations of the disordered ligands are essentially equal. Finally, in an attempt to confirm the above analysis of the disorder problem, we have carried out a crystal structure determination of a *second, independent* crystal of [Fe(T2,6Cl$_2$PP)(1-VinIm)$_2$]ClO$_4$ prepared from the same sample of 1-vinylimidazole. The analysis of this crystal specimen was taken to near completion and gave results that differ immaterially from that of the first crystal.[39] We thus believe that the structural results reported herein are characteristic of all the large crystals obtained from the reaction of [Fe-

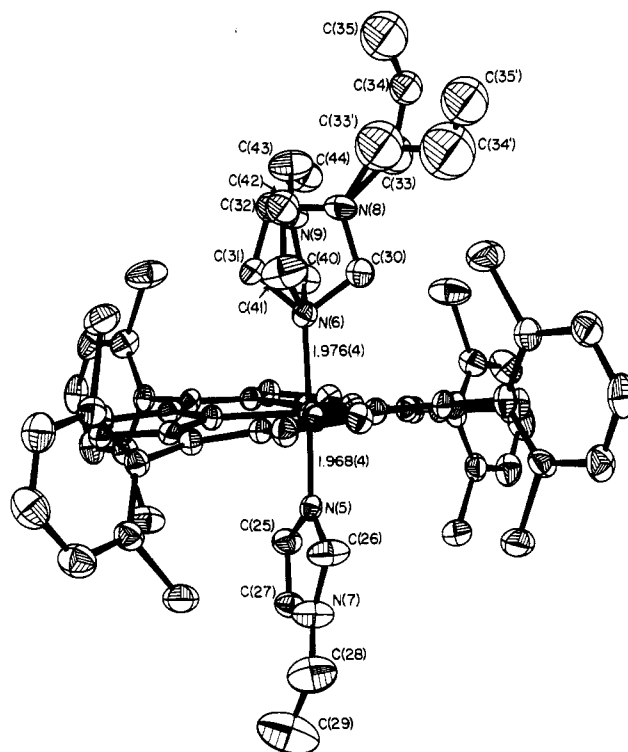(39) Data were collected at 115 K, observed data = 6343, R_1 = 0.078, and R_2 = 0.088; no derived result differs significantly from those of the complete crystal structure determination reported herein.

Figure 5. ORTEP diagram of the [Fe(T2,6Cl$_2$PP)(1-VinIm)$_2$]ClO$_4$ molecule showing the relationship between the three axial ligand orientations. The atom labels of the axial ligands are displayed.

(T2,6Cl$_2$PP)(OClO$_3$)] and 1-vinylimidazole.

The relative orientations of the trans axial ligands for the two types of [Fe(T2,6Cl$_2$PP)(RIm)$_2$]$^+$ molecules are conveniently described as "parallel" and "perpendicular". Figure 3 shows the two axial imidazole ligands of the parallel orientation; the dihedral angle between the two planes is 6°. The side chains of these two imidazoles are completely 1-vinyl substituents. The dihedral angle between the two trans imidazole planes of the nominally perpendicular orientation is 76° (Figure 5). The side chain of this disordered imidazole appears to be largely, if not completely, a three-carbon group. As noted above, the mass spectral analysis of the neat ligand suggests that this impurity contains 14 additional mass units, which could be a propenyl side chain. In our crystallographic analysis of this disorder, we assumed that this side chain was composed solely of three carbon groups rather than a mixture of vinyl and propenyl. Finally, the projections of the three independent imidazole planes onto the porphinato core make angles of 5, 14, and 20° with the closest Fe–N$_p$ vector. As has been noted previously,[40] there appears to be a strong tendency for imidazole ligands in metalloporphyrin species to have orientations where the value of these angles are closer to 0° than to 45°. Thus, although the appearance of two distinct relative orientations of axial imidazoles in the same molecule is unique, the absolute orientations of all are normal.

An examination of the crystal structure reveals an interesting arrangement of the molecules that suggests a possible explanation for the two-orientation disposition of the axial ligands. Figure 6a illustrates the lattice arrangement as projected on the *ab* plane. The two rows of molecules are related by inversion centers between the rows along the *a* direction. Each molecule of the diagram has been drawn with both (disordered) imidazole ligands. The figure shows that there could be seriously short nonbonded contacts between molecules of the two rows. However, these nonbonded contacts can be made reasonable *if* there is a correlation of imidazole orientations between molecules of the two rows. Consider the "origin" molecule labeled A(0) in the figure. This molecule can have two possible relative ligand orientations. If A(0) happens to have a parallel ligand orientation, then impossible nonbonded contacts between the molecule labeled B(0) will occur *unless* B(0) has a perpendicular imidazole orientation. Continuing this alternating pattern to the left yields no serious nonbonded intermolecular interactions, and there is an equal number of molecules with parallel and perpendicular orientations. Now, the molecule labeled B(1) can have either ligand orientation. However, only a perpendicular orientation allows complete freedom of choice at molecule A(1). Eventually, molecules in the two rows to the right will also have alternating relative orientations of the axial ligands. This particular arrangement is schematically illustrated in Figure 6b. In this figure, the solid arrow denotes the (fixed) orientation of the ordered imidazole while the dashed arrow denotes the required orientation (of the two possible) of the disordered imidazole.

Alternatively, if the molecule A(0) is to have a perpendicular ligand orientation, molecule B(1) is required to have a parallel ligand orientation. An alternation of the two ligand orientations in the rows to the right is then necessary to avoid problem nonbonded contacts. Now the molecule at B(0) can take either orientation but eventually the rows to the left must again have the alternating arrangement along the rows as illustrated in Figure 6c. Thus the population of the two orientations along the rows must, on average, become effectively equal. The lattice of crystalline [Fe(T2,6Cl$_2$PP)(1-VinIm)$_2$]ClO$_4$ is entirely made up of such row pairs. There is no apparent way (or more importantly need) to communicate ligand orientation information beyond such row pairs and each row pair is independent of all others.[41] Finally, Figure 6c suggests that the volume available for the imidazole
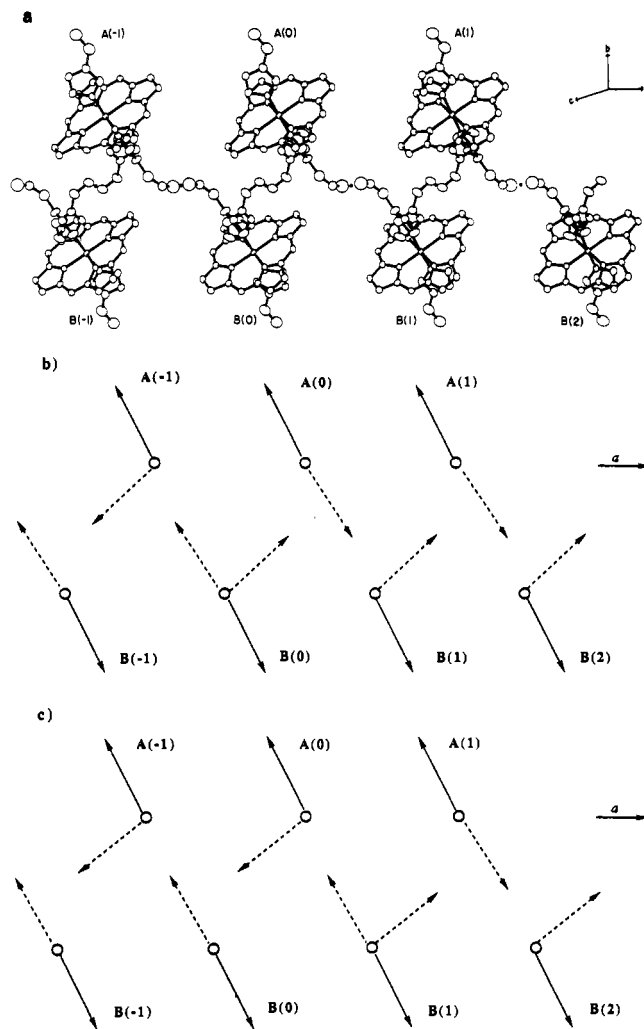
(40) Scheidt, W. R.; Chipman, D. M. *J. Am. Chem. Soc.* **1986**, *108*, 1163–7.
(41) This analysis does not appear to require the consideration of subcell/supercell possibilities. Moreover, a careful photographic examination searching for longer cell dimensions did not suggest the presence of any such phenomena. It should also be noted that the origin molecule A(0) can occur anywhere along a given row pair.

Figure 6. (a) Lattice arrangement of the [Fe(T2,6Cl$_2$PP)(1-VinIm)$_2$]-ClO$_4$ molecules as projected on the *ab* plane. The two rows of molecules are related by the inversion centers shown. (b) Schematic representation of axial ligand orientations required if A(0) has a parallel orientation. (c) Schematic representation of axial ligand orientations required if A(0) has a perpendicular orientation.

side chain is larger for the orientation yielding the perpendicular arrangement. This is a possible explanation of why all of the "impurity ligand" is concentrated in one particular orientation. It is clear that the impurity ligand is concentrated in these crystals to levels well above those in the reagent as used in the crystallization experiment. There is no reason to expect much difference in log β'_2 for the "impurity" ligand compared to 1-vinylimidazole since both are N–R imidazoles. Thus, the concentration of the impurity ligand must be due to the stability of packing in the crystalline state. Indeed, the effect would appear to be one in which a molecular recognition process is occurring in forming the solid-state species.

The crystal structure clearly demonstrates that the two different EPR spectra of crystalline [Fe(T2,6Cl$_2$PP)(1-VinIm)$_2$]ClO$_4$ result from two relative orientations of the axial imidazole ligands in the crystalline solid. Unfortunately, it was not possible to grow large enough crystals of the form that gave only the normal rhombic EPR spectrum to allow a structure determination. The frozen-solution EPR spectrum of [Fe(T2,6Cl$_2$PP)(1-VinIm)$_2$]-ClO$_4$, which shows only a single normal rhombic spectrum, suggests that, in the absence of solid-state packing effects, the parallel orientation is thermodynamically favored, in accord with earlier observations for almost all bis(imidazole)iron(III) porphyrinate complexes in which the imidazole is nonhindered.[8,40] The slight differences in *g* values for the frozen solution as compared to the solid lead to slightly different values of the "tetragonality" and "rhombicity" defined by Blumberg and

Peisach.[23] The tetragonality, Δ/λ, is usually considered to be a measure of ligand donor strength, while the rhombicity, V/Δ, is measure of the degree of splitting of the three d_π orbitals, $(d_{yz} - d_{xz})/[(d_{yz} + d_{xz})/2 - d_{xy}]$. The difference in the values of the tetragonality may suggest differences in medium effects between the frozen solution and the solid state; differences in the rhombicity are consistent with the axial ligand being more closely aligned with the Fe–N$_p$ vector in solution than they are in the solid state.[42]

The value of g_z for the large g_{max} species (3.70), which is larger than that found for [Fe(TPP)(2-MeHIm)$_2$]ClO$_4$,[8] even though the relative orientation of the two ligands is less close to perpendicular (76° rather than 88°[43]), suggests that there is an additional effect due to the orientation of the axial ligand planes with respect to the Fe–N$_p$ vectors. In the present case, the axial ligands are closer to lying over a Fe–N$_p$ vector than in the former, where they were oriented at angles of 41° to those vectors. Thus the perpendicular species of the present crystalline species represents our closest approach thus far to the fourth limiting orientation of axial ligands and prophyrin vectors: perpendicular, with the ligand planes lying over Fe–N$_p$ vectors. The large value of g_z found in this case suggests that the rhombicity may be different from that found for [Fe(TPP)(2-MeHIm)$_2$]ClO$_4$.[8] Assuming $\Sigma g^2 = 16$, $g^2_x + g^2_y = 2.31$. Solving this for $\Delta/\lambda = 3.44$, as found for the normal rhombic species (vide supra), gives $g_x = 0.43$, $g_y = 1.46$, $V/\lambda = 0.53$, and the rhombicity, $V/\Delta = 0.15$. Indeed, this value is only half that found for [Fe(TPP)(2-MeHIm)$_2$]ClO$_4$,[8] suggesting that, in addition to the relative orientation of the two ligands, their absolute orientation with respect to the Fe–N$_p$ axes of the porphyrin is also important. Similar conclusions with respect to the EPR parameters of the normal rhombic species and the orientation of their parallel axial ligands with respect to the porphyrin axes were reached by Strouse and co-workers.[42]

The observed average Fe–N$_p$ bond distance of 1.978 (8) Å is nominally shorter than the 1.990-Å value given by Scheidt and Reed[44] as the canonical value for bisligated iron(III) porphyrinates. The shortened equatorial distances are the result of the core ruffling; as originally noted by Hoard,[45,46] an S_4 ruffling of the core leads to shorter M–N$_p$ bond distances compared to distances in analogous species with planar porphyrin cores. The average axial Fe–N(Im) bond distance is 1.972 (6) Å. This Fe–N(Im)

distance is comparable to the average Fe–N(Im) distances found in the analogous complexes with other unhindered imidazoles: 1.974 (24) Å in [Fe(TPP)(HIm)$_2$]Cl,[47] 1.971 (9) Å in [Fe(TPP)(HIm)$_2$]Cl·CHCl$_3$·H$_2$O,[48] 1.973 (8) Å in [Fe(TPP)(c-MU)$_2$]$^+$,[42] 1.983 (4) Å in [Fe(TPP)(t-MU)$_2$]$^+$,[42] and 1.977 (16) Å in [Fe(Proto IX)(1-MeIm)$_2$].[49] The value is however significantly smaller than the value found in the hindered imidazole complex (with a perpendicular ligand orientation): 2.013 (4) Å in [Fe(TPP)(2-MeHIm)$_2$]ClO$_4$.[43]

In conclusion, we have found that 1-vinylimidazole and an impurity three-carbon-substituted imidazole bind to [Fe(T2,6Cl$_2$PP)(OClO$_3$)] such that two different relative orientations of the two axial ligand planes are produced; those complexes in which both ligands are 1-vinylimidazole have the axial ligands oriented so that their planes are nearly parallel and lie close to one of the Fe–N$_p$ axes. This species gives a normal rhombic EPR signal. Those complexes in which one of the ligands is 1-vinylimidazole and one is the impurity imidazole have their axial ligand planes in nearly perpendicular planes, with one ligand lying fairly close to one of the Fe–N$_p$ axes and the other ligand lying close to the other, and give rise, at very low temperature, to a large g_{max} signal having a higher value of g_z than that for crystalline [Fe(TPP)(2-MeHIm)$_2$]ClO$_4$.[8] This larger value of g_z leads to a calculated rhombicity which is only half that of the previously studied complex and suggests that perpendicular alignment of axial ligand planes *close* to the two Fe–N$_p$ axes produces the smallest splitting of the d_{xz} and d_{yz} orbitals. The axial bis(imidazole) complexes of the so-called hindered porphyrin [Fe(T2,6Cl$_2$PP)(OClO$_3$)] are considerably more thermodynamically stable in solution than those of [Fe(TPP)Cl].

(42) Quinn, R.; Valentine, J. S.; Byrn, M. P.; Strouse, C. E. *J. Am. Chem. Soc.* **1987**, *109*, 3301–8.

(43) Scheidt, W. R.; Kirner, J. F.; Hoard, J. L.; Reed, C. A. *J. Am. Chem. Soc.* **1987**, *109*, 1963–8.

(44) Scheidt, W. R.; Reed, C. A. *Chem. Rev.* **1981**, *81*, 543–55.

(45) Hoard, J. L. *Ann. N.Y. Acad. Sci.* **1973**, *206*, 18–31.

(46) Collins, D. M.; Scheidt, W. R.; Hoard, J. L. *J. Am. Chem. Soc.* **1972**, *94*, 6689–96.

(47) Collins, D. M.; Countryman, R.; Hoard, J. L. *J. Am. Chem. Soc.* **1972**, *94*, 2066–76.

(48) Scheidt, W. R.; Osvath, S. R.; Lee, Y. J. *J. Am. Chem. Soc.* **1987**, *109*, 1958–63.

(49) Little, R. G.; Dymock, K. R.; Ibers, J. A. *J. Am. Chem. Soc.* **1975**, *97*, 4532–9.